[1963]

38p refs

Code 2A

(NASA TMX 51008)

[7] conf.

INVESTIGATION OF SOME NEW MATERIALS FOR AEROSPACE VEHICLE APPLICATIONS

By C. R. Manning, Jr. and E. E. Mathauser

NASA Langley Research Center,
Langley Station, ~~Hampton,~~ Va.

Presented at the ~~Sixth~~ 6th Natl~~ional~~ l. SAMPE Symp~~osium~~,

Seattle, ~~Washington~~
Nov~~ember~~ 18-20, 1963

INVESTIGATION OF SOME NEW MATERIALS FOR AEROSPACE VEHICLE APPLICATIONS

By C. R. Manning, Jr.* and E. E. Mathauser**
NASA Langley Research Center

SUMMARY

17043

The highlights of several studies at the Langley Research Center of the NASA to determine potential utilization of recent new materials for aerospace vehicle applications are presented. The materials are reviewed in terms of possible use in nose and leading edges, external heat-shield surfaces, and primary load-carrying structures. For the most severely heated portions of aerospace vehicles, the performance of JTA graphite, porous oxide ceramics, and a Cr-MgO cermet are reviewed. Significant test results from thoriated nickel and vanadium-base alloys that may find use for external surfaces and for primary structure are reported. The role of beryllium produced by plasma spraying for structural and heat-sink applications is briefly indicated. Significant material properties, metallurgical characteristics, and fabrication capabilities are discussed with particular reference to desirable properties and notable deficiencies.

AUTHOR

INTRODUCTION

The severe environments associated with different aerospace vehicles have created a need for greatly improved materials for use in the structure and thermal-protection systems. As a result of this need, the materials community is constantly introducing many types of new or improved materials to cope with the new environments. Frequently very little material property data and test

*Aerospace Technologist.

**Head, Structural Materials Branch.

L-3601

experience are reported to assess the potential usefulness of the proposed material. In order to establish the characteristics and to categorize these new or improved materials, the Langley Research Center of the NASA has been pursuing investigations that include mechanical, physical, and chemical property determinations, metallurgical evaluation, fabrication, and joining studies. The studies are expected to aid in determining significant properties and whenever possible the materials deficiencies.

In this paper, only the highlights of several studies on metallic, ceramic, or metal-ceramic compositions will be presented. These types of materials may be useful under moderate heating conditions associated with lifting reentry vehicles. Ablation materials that are tailored to operate in the thermal-protection systems of ballistic or low-lifting-type vehicles will not be included. Six relatively new or heretofore unexplored materials will be discussed. These materials are noted in figure 1.

Three materials, namely JTA graphite, porous oxide ceramics, and Cr-MgO cermet, will be discussed with regard to possible applications in the stagnation areas (such as nose caps and leading edges) of aerospace vehicles. The usable temperature range for these materials would probably extend above 2,500° F.

Nickel containing dispersed thoria, commercially known as thoriated or TD nickel, and newly developed vanadium alloys are considered to have potential application in thermal-protection systems involving metallic heat shields and in the hot primary load-carrying structure of the vehicle. The useful temperature range for these materials would probably be from approximately 1,500° F to 2,500° F.

The last material noted is plasma-sprayed beryllium. This material has been frequently considered to be a potentially useful material although little

information on its structural characteristics is available. Plasma-sprayed beryllium would be limited in use for load-carrying structures to temperatures below approximately 800° F and for heat-sink, nonstructural application the maximum usable temperature would probably be in the vicinity of 1,500° F.

RESULTS OF INVESTIGATIONS

JTA Graphite.- Although many types of commercial graphites are available, relatively little use has been made of this material in either load-carrying or thermal-protection systems. Graphite possesses several outstanding desirable characteristics such as high-temperature strength, good thermal shock resistance, and high melting point; however, several notable deficiencies also exist, among these its brittleness and poor oxidation resistance. Several types of coatings for graphite have been studied for oxidation protection and to date no generally satisfactory coating is available.

A recent advance in the development of graphite is of interest. This advance is in the form of a new graphite (ref. 1) which is commercially known as JTA and consists of graphite to which zirconium diboride and silicon have been added. This composite material is expected to provide its own oxidation-resistant coating during exposure at high temperatures. In order to evaluate the performance of this type of material, the Langley Research Center has been conducting both static and dynamic oxidation tests on the JTA graphite.[1] The results of the static oxidation tests indicate that the material has the capability to form a protective coating to reduce the oxidation of the graphite. The weight losses established from tests in a static oxidizing atmosphere for the JTA graphite are

[1]The preliminary data reported herein were obtained by Donald R. Rummler of the Structures Research Division, NASA Langley Research Center.

generally 20 to 30 times less than the weight losses obtained from other commercial graphites at corresponding temperatures.

The performance of the JTA graphite under dynamic oxidation conditions also appears to be greatly improved as compared with standard graphite. In figure 2 a JTA graphite specimen is shown under test in the 2,500 kw arc jet at the Langley Research Center. At the left is shown a standard ATJ graphite specimen after 3 minutes of exposure in this arc jet at a free-stream temperature of approximately 3,500° F. A weight loss of over 50 percent occurred. This large weight loss is an indication of the rapid surface recession produced by oxidation. The specimen shown on the right is the new composite graphite JTA after a total of 24 minutes exposure in the arc jet. A weight loss of approximately 5 percent occurred during this total test time. The 24 minutes total test time was obtained from 4 separate tests of the same specimen. The protective layers that formed on the surface spalled slightly during these cyclic heating tests but the magnitude of weight change was very low in contrast to that obtained with the standard ATJ graphite.

A complete understanding of the mechanism that protects the JTA graphite during dynamic oxidation testing has not been obtained to date; however, it appears that some of the protection is derived from zirconia that forms on the surface. The role of silicon and boron in the oxidation protection mechanism is not completely established. More evaluation tests of this composite graphite are required before it can be firmly established as a significant aerospace material. The available experience, however, suggests that the material has definite promise, although data have not yet been obtained on the mechanical properties.

Porous oxide ceramics.- Porous oxide ceramics such as alumina, zirconia, or hafnia have been considered for use in the thermal-protection systems of certain

aerospace vehicles (refs. 2 and 3). Figure 3 shows a typical porous ceramic. This material is zirconia with approximately 85-percent voids. The zirconia has a high melting point of approximately 4,800° F, possesses good oxidation resistance, low thermal conductivity, and contains interconnecting pores that permit impregnation of the ceramic with ablation materials or passage of materials for transpiration cooling. Utilization of this material in heat shields involves attaching the ceramic to the metal substructure by adhesives or other bonding materials. When the porous ceramic is subjected to external heating, the low melting materials contained in the pores transpire through the interconnected pores and provide the necessary cooling for the vehicle. Little if any surface recession would be anticipated with this type of system and consequently no important changes in aerodynamic performance of the vehicle would be experienced. In addition, the ceramic matrix remaining after the ablation process is completed provides a relatively good insulator between the externally heated surface and the cooler internal structure because of its low thermal conductivity. The ceramic may also provide a coating for protection of the structure from oxidation.

One of the principal deficiencies of this thermal-protection system appears to be the temperature limitation imposed by the adhesive used for attachment of the porous ceramic to the metallic structure. Relatively low temperatures must be maintained at the bond line to prevent separation of the ceramic shield from the metallic structure. In order to permit higher bond line temperatures a limited study was undertaken to investigate several methods of attaching porous ceramics to metals.

The efforts to join the ceramic to metal were based on establishing a graded material between the metal and ceramic to give compatibility of thermal expansion

coefficients.[2] One of the efforts consisted of spraying the porous ceramic (alumina in this case) with alumina powder to establish a dense surface. The ceramic surface was then plasma sprayed with successive layers of tungsten, molybdenum, columbium, and nickel in various combinations. This combination was next vacuum brazed at approximately 2,000° F to the metallic sheet using nickel braze alloys. A parallel effort was made using an expansion graded combination of nickel and alumina. This mixture was sprayed on the structural sheet (René 41) starting with pure nickel and increasing the alumina content until 100-percent alumina was obtained on the outer layer. Silica was used to join this composition to the ceramic.

A somewhat different approach is shown in figure 4 which consists of introducing a low-density metal matrix (on the order of 5 percent of theoretical density) between the ceramic and the metal structure. The low-density metal layer was selected to provide a low-bulk-modulus filler material between the structural metal and the porous ceramic.

The various approaches outlined appear to show some promise for attachment of the ceramic to the metal; however, the assembly usually fails during the cooling portion of the brazing or bonding cycle because of the low shear strength of the porous ceramic. An assessment of the results obtained to date indicates that the porous ceramic does not hold much promise as a heat-shielding material until major improvements are obtained in its mechanical strength properties.

Cr-MgO cermet.- A composite of chromium and magnesium oxide has become available recently as a possible aerospace material for high-temperature use

---

[2]The preliminary data reported herein were obtained by William H. Herrnstein III of the Structures Research Division, NASA Langley Research Center.

(ref. 4). This material, shown in figure 5, consists of a high percentage of chromium with 5- to 20-micron-sized magnesium-oxide particles dispersed uniformly throughout. This metal-ceramic composite was reported to possess good room-temperature ductility and to be usable at high temperatures without coatings for oxidation protection. No data were available on the performance of this cermet material in sheet form. For this reason, a preliminary investigation was made to obtain such data for 0.020-inch-thick sheet (ref. 5). This material thickness was selected to compare favorably on a weight-per-square-foot basis with minimum gage sheet of molybdenum or columbium considered for aerospace vehicles. The results of tensile tests are shown in figure 6 where the tensile and yield strength as well as the elongation in a 1-inch gage length are plotted against temperature to 2,500° F. The elevated-temperature results were obtained by testing immediately after reaching the test temperature. The tensile results show the strength values are low at elevated temperature, but it appears that this material may be useful in lightly loaded areas such as the leading edge or nose applications.

An examination of the oxidation properties of the cermet was also included in the investigation. Curves showing the oxidation test results are given in figure 7. In this figure the material recession produced by oxidation is plotted against test time. Note that at 2,800° F the 0.020-inch-thick sheet would be completely destroyed in less than 3 hours if oxidation occurred from both sides although this is not the case at 2,000° F. Although the loss of material due to oxidation is rapid, an embrittling mechanism was noted during elevated-temperature exposure that overshadows the loss of material due to oxidation. This embrittling effect can be seen in figure 8. On the left is a micrograph of the material exposed at 2,000° F for 4 hours, and on the right is a micrograph of the sheet

after an exposure of 4 hours at 2,500° F. The numerous straight lamellar precipitates that appear in the grains and grain boundaries in the right-hand figure are evidence of nitrogen penetration into the material. The nitrogen combines with the chromium to form chromium nitride Cr_2N which produces embrittlement. This nitrogen penetration into the material was found to be approximately five times greater than the loss of material due to oxidation above 2,200° F. This nitrogen embrittlement reduced the elongation to approximately zero and changed the cermet from a ductile to a brittle material.

The chromium cermet sheet also appeared to be embrittled by another entirely different mechanism. It was noted that small surface scratches changed the material from an apparently ductile material at room temperature to a brittle material. This type of embrittlement is frequently indicative of high chromium base alloys. This behavior would be particularly undesirable if use were made of the material without frequent inspections for surface scratches.

Our test results on the cermet sheet indicate that the sheet oxidizes too rapidly above 2,400° F to be of interest in thin gages. The embrittling effect of nitrogen and the sensitivity to small scratches and surface conditions further make the material marginal for aerospace use in sheet form. Use of the material in thicker sections may possibly overcome some of these deficiencies.

Thoriated nickel.- A recently developed nickel containing approximately 2-percent thoria (known as thoriated nickel or TD nickel) has received considerable attention recently (refs. 6 and 7). An electron micrograph of the material is shown in figure 9. The material consists of nickel with a uniform dispersion of submicron-sized thoria. The thoria acts as an effective strengthening agent for the nickel at elevated temperatures by blocking grain boundary and dislocation movement. Elevated-temperature tensile properties are shown in figure 10

where the tensile and yield strengths and elongation are plotted against temperature. The room-temperature tensile strength is approximately 80 ksi and the elongation is approximately 15 percent. The elevated-temperature strength decreases to 4,100 psi at 2,500° F. This temperature is within 150° F of the melting point of the material.

Studies were also conducted to establish the oxidation characteristics of the thoriated nickel. Some of the data obtained in the investigation are shown in figure 11. The weight gain is plotted against test temperature. Results are shown for uncoated thoriated nickel and for aluminide-coated thoriated nickel (calorizing process) at 10 and 100 hours. The calorizing coating proved very effective in reducing weight gain due to oxidation. Even though the nickel material is not exceptionally resistant to oxidation, it should be noted that no grain boundary oxidation occurs as is frequently noted in precipitation-strengthened nickel-base superalloys considered for high-temperature use. This result is very significant because the loss of strength can be attributed only to surface recession. Embrittlement associated with grain boundary oxidation is not obtained even after prolonged exposure at 2,500° F.

Various types of fabrication and joining methods were investigated to determine the ability of the TD nickel to be formed and joined into useful structural configurations. The types of welding methods that were studied included electron beam, tungsten inert gas, and resistance welding. Of these, the resistance welding produced the least amount of agglomeration of the thoria. Diffusion bonding was also investigated. Small sandwich panels joined by diffusion bonding are shown in figure 12. The sandwich panels consist of alternate layers of flat and dimpled sheets. In the left-hand view the thoriated-nickel sheet was 25 mils thick. In the right-hand view the dimpled sheets were 2 mils thick, the external

face sheets 10 mils, and the interior flat sheets 4 mils thick. Excellent joints were obtained by diffusion bonding. The specimens were encapsulated in a small metal retort and evacuated to about 10^{-4} torr by a pumping system consisting of a mechanical and a diffusion pump. The sandwiches were then subjected to a bonding temperature of 2,000° F for 24 hours. One of the bonded joints between the face sheet and dimpled sheet is shown in figure 13. This figure shows the dimpled sheet in the upper half and the flat face sheet in the lower half. Both sheets were 25 mils thick. An excellent bond was obtained. No evidence of agglomeration of the thoria was detected.

The TD nickel, developed by the E. I. DuPont De Nemours and Co., is undergoing further improvements. A recent modification revealed by the company which is in the latter stages of development consists of a molybdenum addition to the thoriated nickel. The molybdenum is added as a solid solution strengthening agent. Preliminary test results reported by the company's research laboratory indicate a significant strength increase at room temperature from 80 ksi to 115 ksi and at 1,200° F from 30 ksi to 65 ksi. The 100-hour rupture strengths at 1,600° F to 1,900° F are approximately doubled (15,000 to 25,000 psi and 9,000 to 15,000 psi, respectively). Preliminary results indicate that the molybdenum modified thoriated nickel is much stronger than ordinary TD nickel to 1,900° F and above this it is at least as strong to 2,500° F. In addition, no degradation of the oxidation resistance found in the unmodified TD nickel is obtained with the newer material.

The assessment of test experience suggests that thoriated nickel is a material with considerable promise for aerospace vehicle applications. Further improvements in the material are expected and such improvements should make its potential use even more promising.

Vanadium alloys.- Vanadium alloys are receiving attention as structural materials because of the potentially outstanding characteristics in the 1,800° F to 2,400° F temperature range. The limited data available in the literature suggested that in this temperature range the vanadium alloys on a strength-weight basis would be the optimum materials for construction (ref. 8). Because of this potential as a structural material, NASA as well as other governmental and industrial organizations are undertaking a preliminary evaluation of several vanadium alloys produced by the Armour Research Foundation of the Illinois Institute of Technology for the Bureau of Naval Weapons (ref. 9).

Two alloys of vanadium that merit attention have been produced to date. These are noted in figure 14 which shows a typical microstructure of the V-60 w/o Cb alloy. The composition and density of the 20 w/o columbium, 4 w/o Ti, and 1 w/o Zr are shown on the left, and on the right are those of the 60 w/o columbium and 1 w/o titanium alloy. The density of the alloy on the left is 0.228 pound per cubic inch and that on the right is 0.268 pound per cubic inch. Both of these alloys are undergoing evaluation tests in various organizations at the present time.

The elevated-temperature tensile properties of these alloys are shown in figure 15. The strengths of both alloys are shown plotted against temperature to 2,400° F. Elongation is shown for the 20 w/o columbium alloy but the measurements were not obtained for the other alloy. The vanadium alloy containing 60 w/o columbium shows higher strength values than the 20 w/o columbium alloy over the entire temperature range. This result is expected because columbium has greater elevated-temperature strength than vanadium. One potential disadvantage is suggested by the high elongation of the material above 2,200° F. This

elongation of over 100 percent generally indicates poor long-time strength and creep properties.

Oxidation tests were made on the uncoated vanadium alloys at 1,800° F and 1,950° F. These results are shown in figure 16. The surface recession is plotted against time. Both alloys display poor resistance to oxidation, even at 1,800° F and thus coatings for protection against oxidation are required. The material loss at 1,800° F is almost twice as great for the 20 w/o columbium alloys as that for the 60 w/o columbium. The large percentage of columbium appears to retard the oxidation appreciably.

Both alloys were coated with a silicide-type coating to protect the metal against the rapid oxidation (ref. 10). The results of the static oxidation tests for the 60 w/o columbium alloy are given in figure 17. The change in weight of coated specimens expressed on a percentage basis is plotted against time. Results are shown for a silicide coating at three test temperatures. A pure silicide coating appears to protect the 60 w/o columbium alloy satisfactorily to temperatures of 2,400° F during static oxidation testing, but above this temperature the coating is not reliable. Essentially the same results were found during cyclic oxidation testing. Initial work on the 20 w/o columbium alloy indicates that the same coating does not afford protection to the material above 2,000° F and that modification to this coating must be made if the material is to be used above this temperature.

In addition to these studies, joining, machining, and forming operations were carried out on both alloys. Machining and forming operations were accomplished with relative ease on the alloy containing 20 w/o columbium. Considerable difficulty was encountered in milling the alloy containing 60 w/o columbium. Joining efforts including tungsten inert gas and electron beam welding were made

with generally excellent results. Tests on butt welds at 2,000° F, for example, gave strengths that were approximately 75 percent of the original material strength at that temperature.

Although only limited amounts of the vanadium-alloy material have been available to date, the test results suggest that some additional improvements are needed in the basic alloys to enable vanadium alloys to find their place as useful high-temperature structural materials. Their low resistance to oxidation, difficulty in machining some of the highly alloyed sheet materials, and suspected poor creep properties are specific deficiencies that should receive attention in further development efforts on the material. Some efforts are currently underway at the Illinois Institute of Technology to improve long-time properties of the material by dispersion strengthening.

Plasma-sprayed beryllium.- In spite of the fact that beryllium possesses the highest stiffness-density ratio available with any structural material, its use in structures has been very limited to date (refs. 11 and 12). Brittleness, toxicity, high cost, and fabrication difficulties are major deterrents to its use. In order to circumvent some of these difficulties, plasma-sprayed beryllium has frequently been mentioned as a possible approach to the use of the metal. Plasma-sprayed beryllium would possibly eliminate many of the forming and joining problems that exist with the use of more conventional mill products. If feasible, this approach might also reduce the cost of making complex structural components.

In order to determine the feasibility of plasma spraying and to establish some of the characteristics of plasma-sprayed beryllium, a preliminary investigation was undertaken.[3] Some of the specimens that were produced during the course

[3]This preliminary work was done by D. R. Rummler of the Structures Research Division, NASA Langley Research Center.

of this study are shown in figure 18 which shows beryllium specimens produced for NASA by plasma spraying. The tensile specimen labeled A shows the as-sprayed outside surface. The specimen labeled B shows the inside or back surface. The third specimen labeled C was produced by plasma spraying and sintering followed by surface grinding to achieve uniform thickness to permit tensile testing. The hollow cylinder labeled D was produced by plasma spraying followed by gas pressure consolidation. No attempt was made to grind the surfaces of specimens A, B, and D. Some variations in thickness existed in these specimens and for this reason they were not utilized in strength tests.

The microstructure of the sprayed beryllium is shown in figure 19. The photomicrograph on the right shows the plasma-sprayed material (500×) and on the left is shown a conventional beryllium sheet. Note that the plasma-sprayed beryllium displays a random structure. Inclusions and porosity not evident in the cast material exist in the plasma-sprayed material. The density of the plasma-sprayed beryllium is approximately 95 percent of the theoretical density after sintering.

Tensile stress-strain results obtained from the plasma-sprayed and sintered specimens and for the QMV material are shown in figure 20. Stress is plotted against strain. The solid curve was obtained from published results on the QMV material (ref. 11). The yield strength on the dashed curve for the plasma-sprayed and sintered material appears to be higher (48,700-psi yield strength as against 33,000-psi yield strength for the QMV material). The study of plasma-sprayed beryllium indicates that porosity and foreign inclusions appear to be detrimental to the tensile properties of the material. Use of the plasma-sprayed beryllium for load-carrying structural elements looks promising but will require

further investigation before its role in aerospace structures is clearly defined. Its potential use for heat-sink applications also requires further study.

CONCLUDING REMARKS

In conclusion, a preliminary investigation of six materials for possible application in aerospace vehicles has been made at Langley Research Center. The investigation indicates that some of the materials exhibit promise for use in hot structures and thermal-protection systems; however, most of the materials have deficiencies that should be eliminated before the materials may be expected to find greater use in aerospace vehicles.

REFERENCES

1. Gibeaut, W. A., and Maykuth, D. J.: Summary of the Sixth Meeting of the Refractory Composites Working Group. DMIC Rep. No. 175, Batelle Memorial Institute, September 24, 1962, pp. 31-32.

2. Strauss, Eric L.: Structural and Heat Transfer Characteristics of Resin Impregnated Porous Ceramics. American Ceramic Bulletin, Vol. 42, No. 8, August 1963, pp. 444-447.

3. Chapman, Andrew J.: An Experimental Evaluation of Three Types of Thermal Protection Materials at Moderate Heating Rates and High Total Heat Loads. NASA TN D-1814, 1963.

4. Scruggs, David M.: Modified Chromium for Unprotected Structures Over 2,600° F (Preprint) 1688-61, American Rocket Society, April 1961.

5. Manning, Charles R., Jr., and Royster, Dick M.: Investigation of Mechanical Properties and Metallurgical Characteristics of a Metallic Chromium and Magnesium Oxide Composite. NASA TN D-1785, 1963.

6. Anders, Fred J., Jr., Alexander, Guy B., and Wartel, William S.: A Dispersion-Strengthened Nickel Alloy. Metal Progress, Vol. 82, No. 6, December 1962, pp. 88-91, 118-122.

7. Manning, Charles R., Jr., and Royster, Dick M.: An Investigation of A New Nickel Alloy Strengthened by Dispersed Thoria. NASA TN D-1944, 1963.

8. Wlodek, S. T.: The Properties of Vanadium-Columbium Alloys. Journal Electrochemical Society, Vol. 107, 1960, pp. 923-929.

9. Rajala, B. R., and VanThyne, R. J.: Improved Vanadium-Base Alloys. ARF 2191-C, Final Report, Armour Research Foundation of Illinois Institute of Technology, Contract Now 61-0417-C for Dept. of Navy, Bureau of Naval Weapons, December 27, 1960.

10. Anon.: Temperature Oxidation Protective Coatings for Vanadium-Base Alloys. ARF-B6001-1,2,3,4, Armour Research Foundation of Illinois Institute of Technology, Contract N600(19) 59182, Dept. of Navy, Bureau of Naval Weapons, September 1962 - May 1963.

11. Hodge, Webster: Beryllium for Structural Applications. DMIC Rep. 106, Batelle Memorial Institute, August 15, 1958.

12. Crawford, Robert F., and Burns, A. Bruce: Strength Efficiency and Design Data for Beryllium Structures. ASD, Technical Report 61-692, Feb. 1962.

MATERIAL	APPLICATION	TEMP. RANGE
JTA GRAPHITE POROUS OXIDE CERAMIC Cr-MgO CERMET	NOSE CAP, LEADING EDGES	ABOVE 2500 °F
TD-NICKEL VANADIUM ALLOYS	HEAT SHIELDS, HOT STRUCTURE	1500 °F TO 2500 °F
PLASMA-SPRAYED BERYLLIUM	PROTECTED STRUCTURE HEAT SINK	TO 800 °F TO 1500 °F

NASA

Figure 1.- New materials for aerospace vehicle applications.

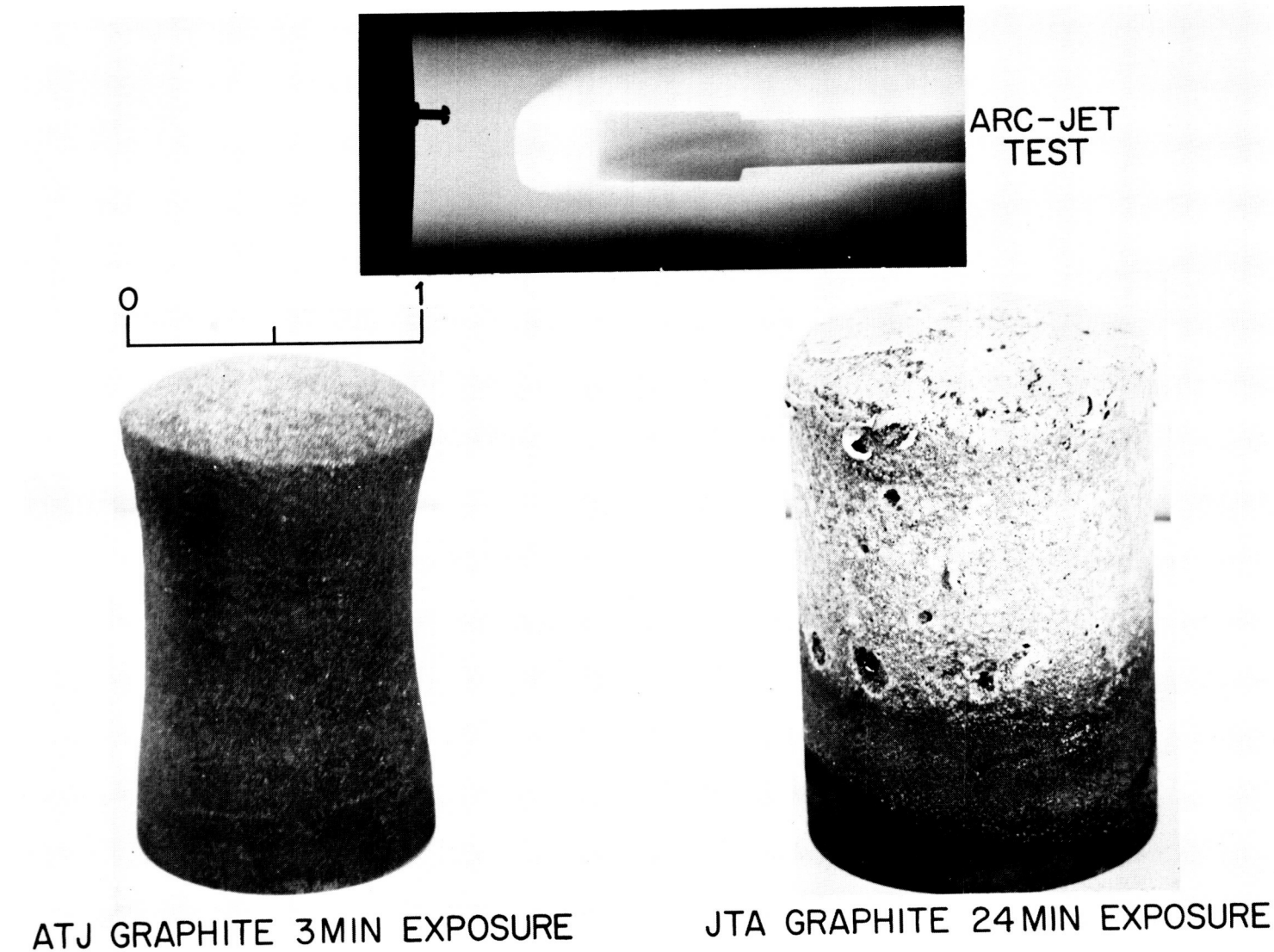

Figure 2.- Comparison of two graphite materials.

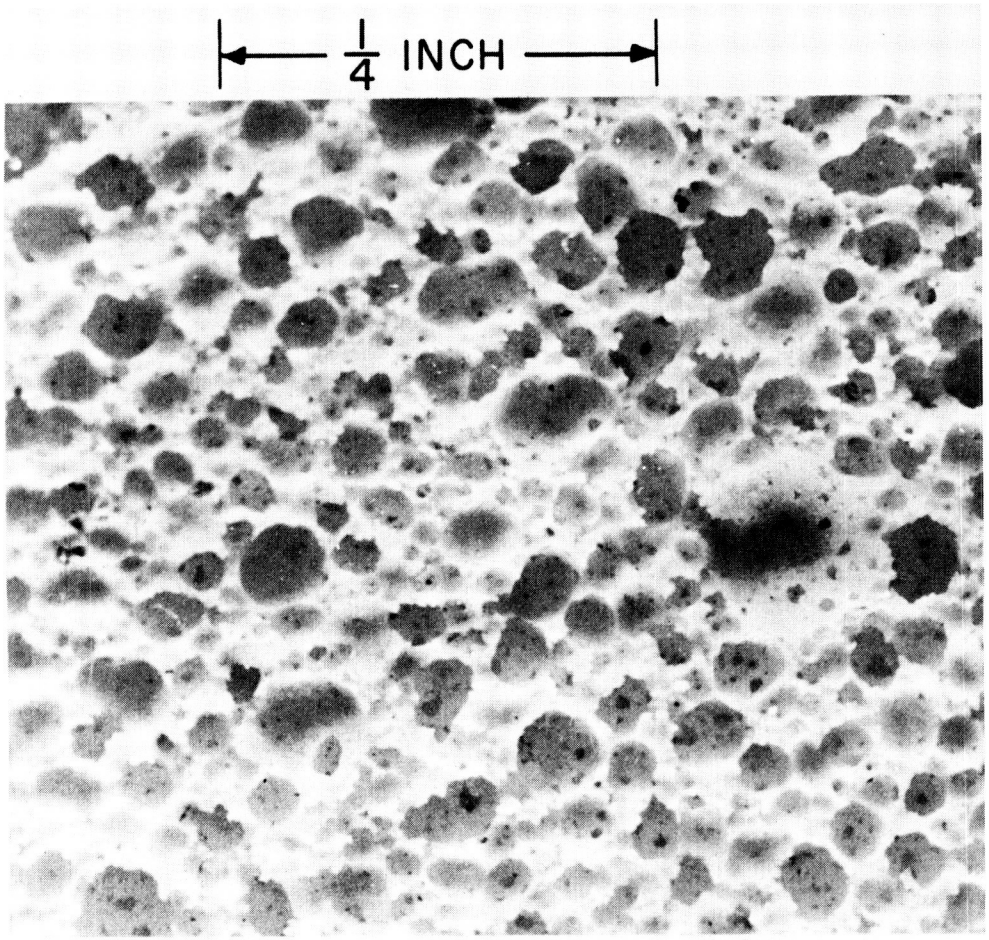

NASA

Figure 3.- Porous oxide ceramic.

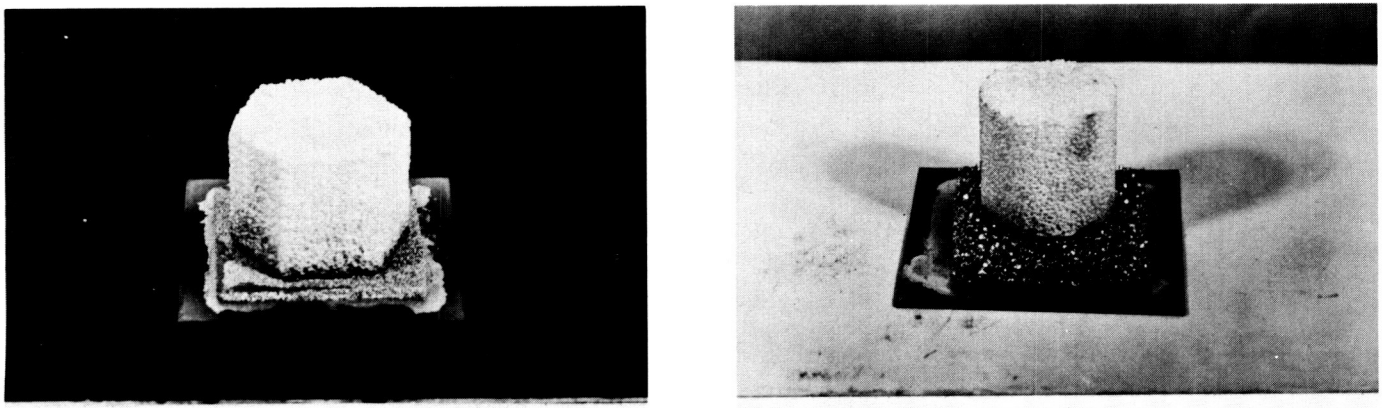

NASA

Figure 4.- Joining porous oxide ceramic to nickel.

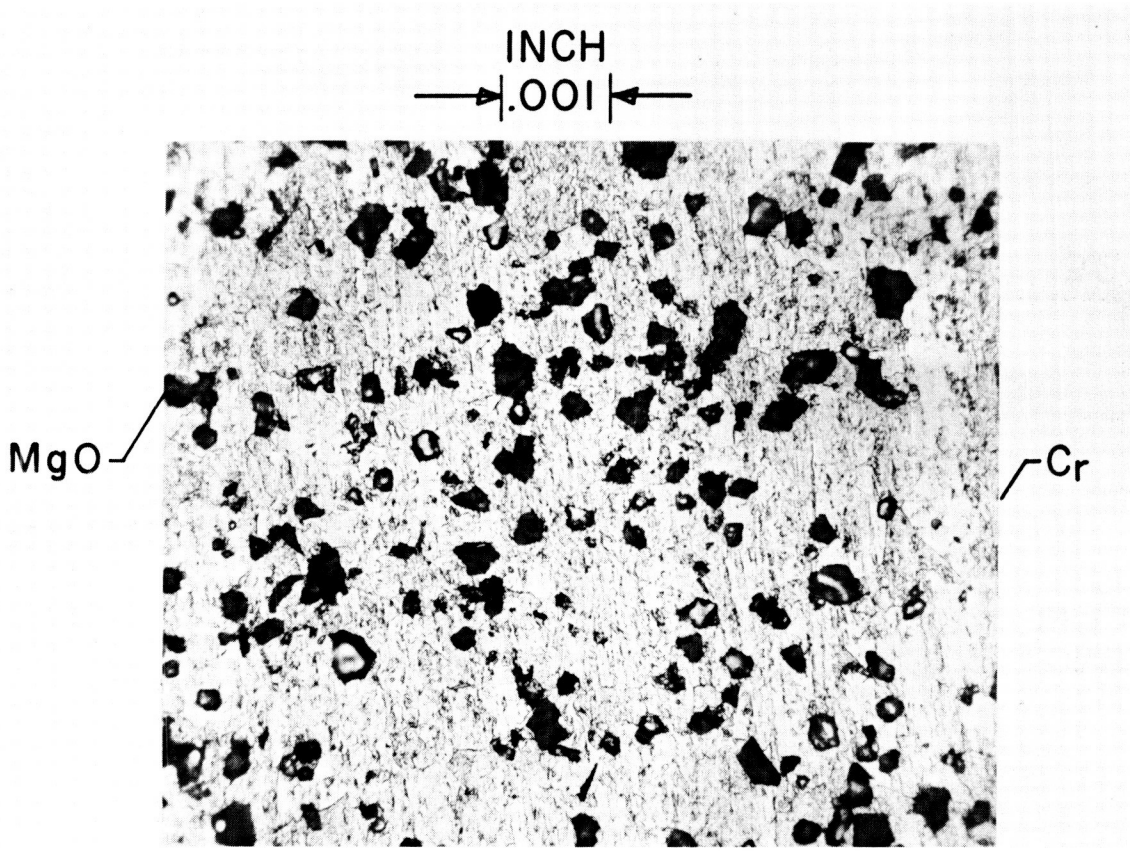

NASA

Figure 5.- Microstructure of Cr-MgO sheet, 500×.

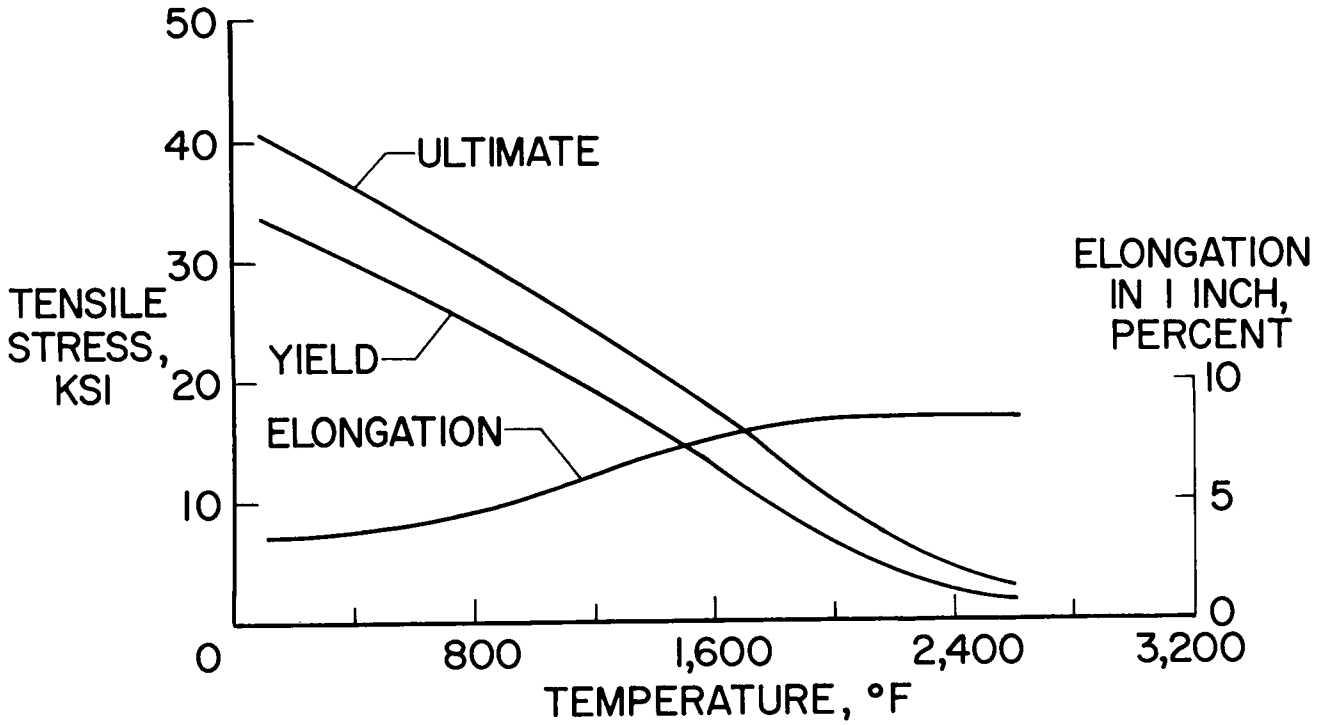

NASA

Figure 6.- Mechanical properties of Cr-MgO cermet.

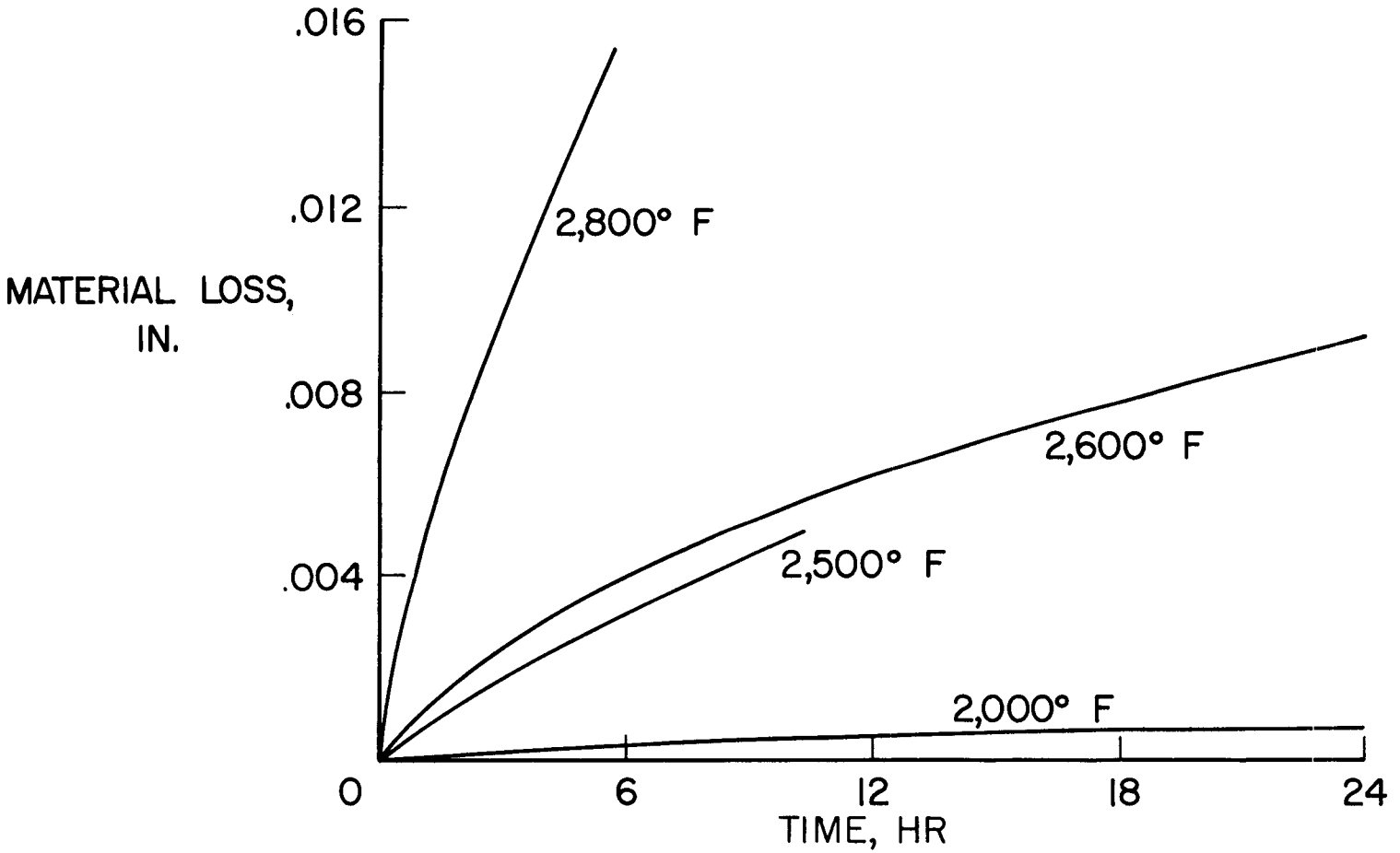

Figure 7.- Oxidation properties of uncoated Cr-MgO cermet.

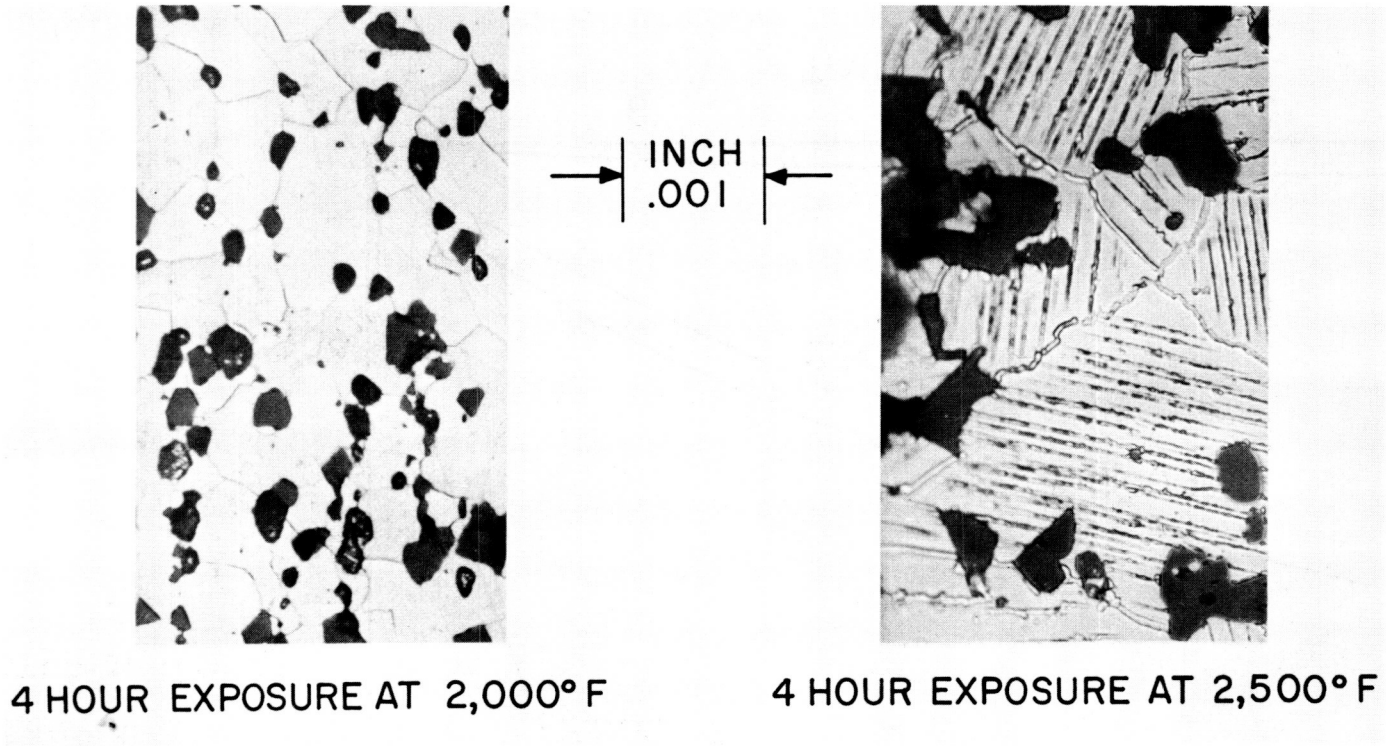

NASA

Figure 8.- Microstructure of Cr-MgO, 750×.

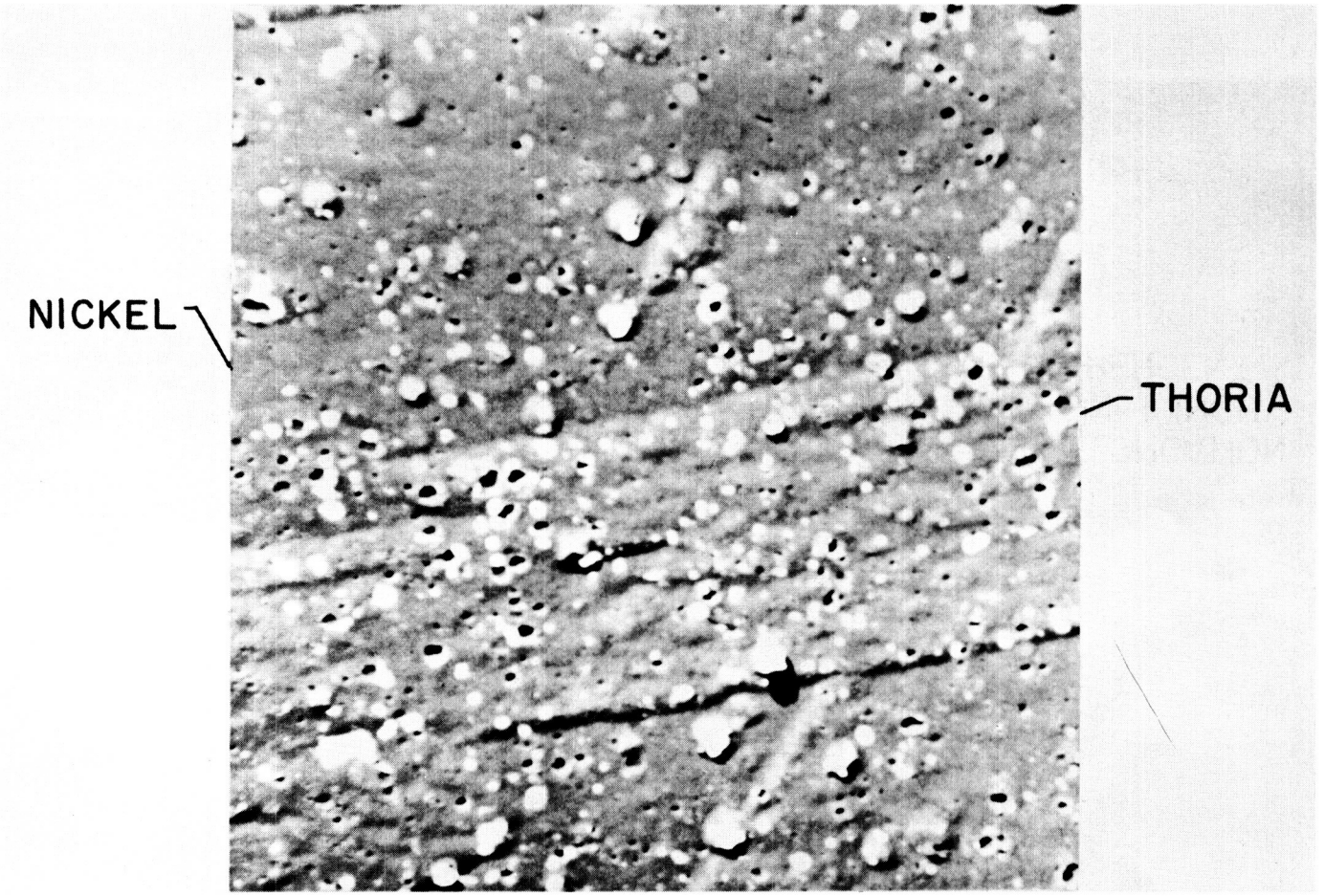

NASA

Figure 9.- Electron micrograph of TD-nickel, 10,000×.

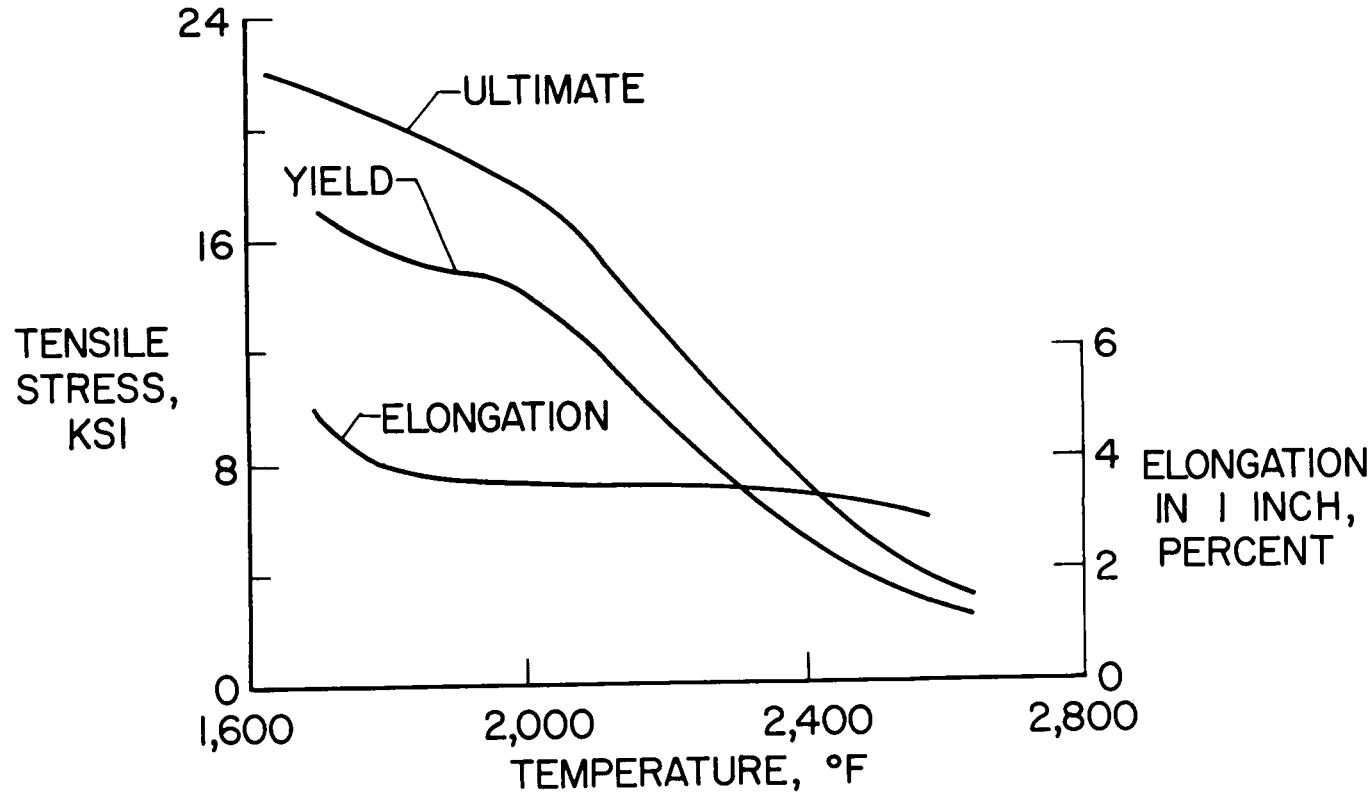

NASA

Figure 10.- Mechanical properties of TD-nickel.

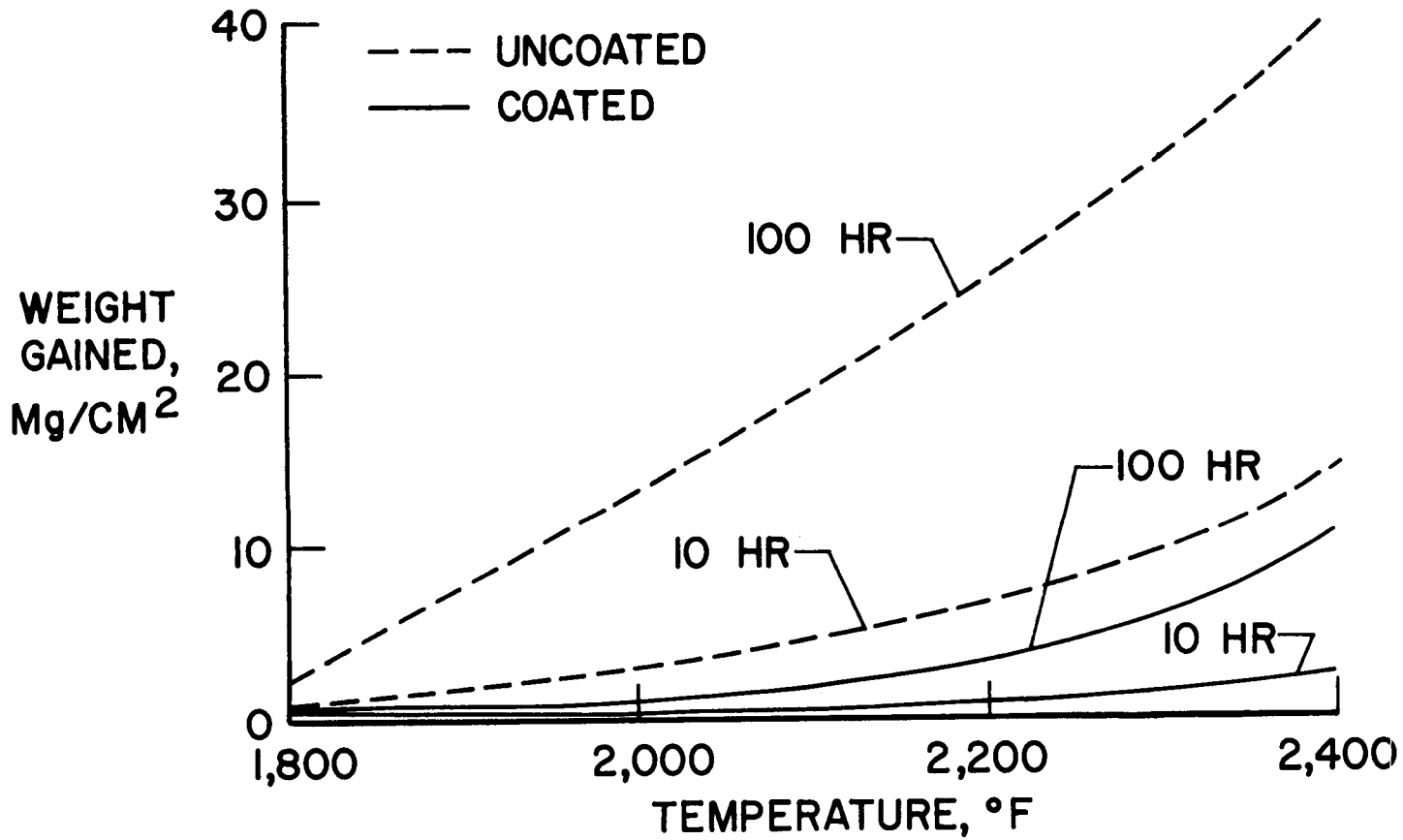

NASA

Figure 11.- Oxidation properties of TD-nickel.

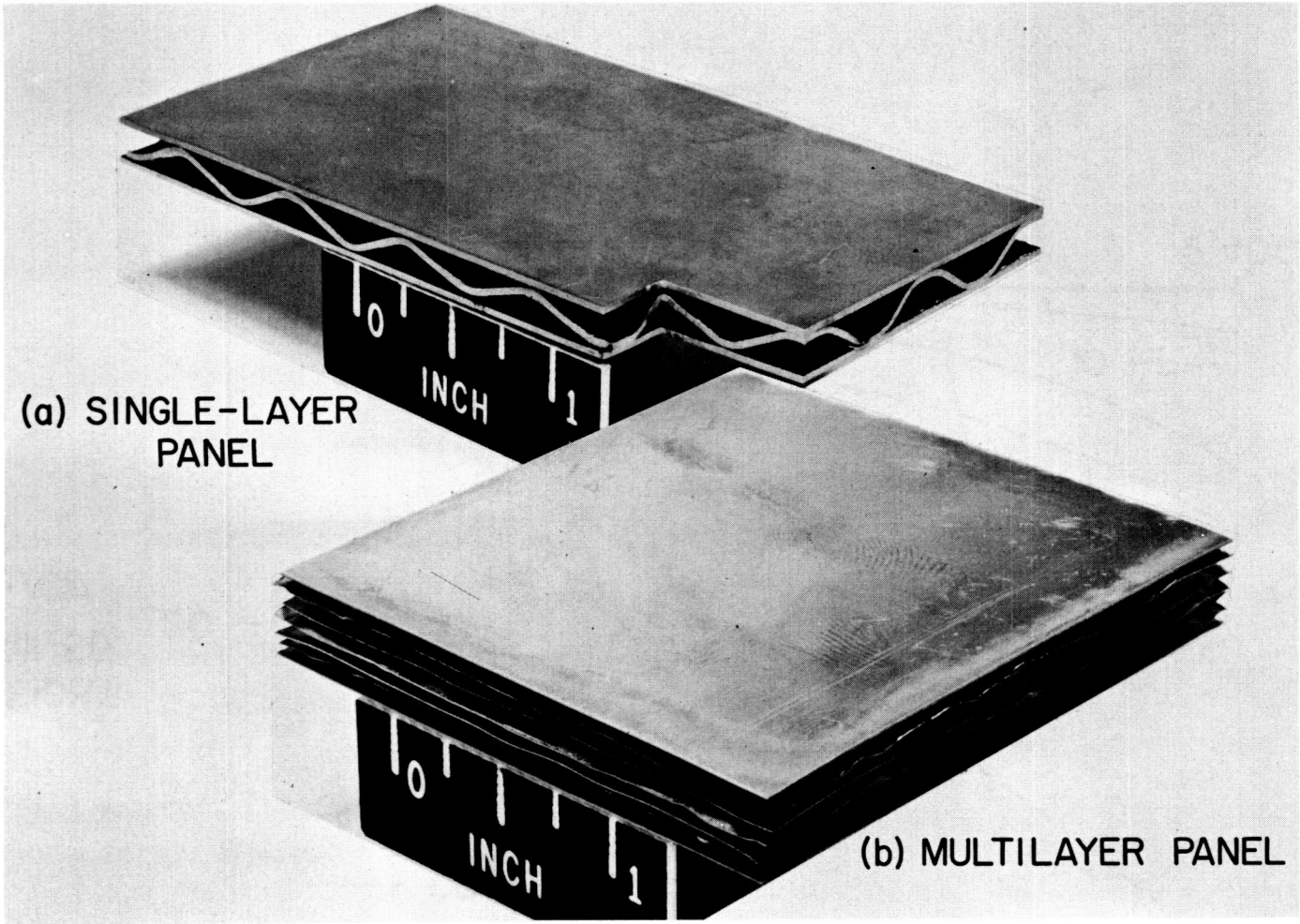

NASA

Figure 12.- Diffusion-bonded sandwich panels of TD-nickel.

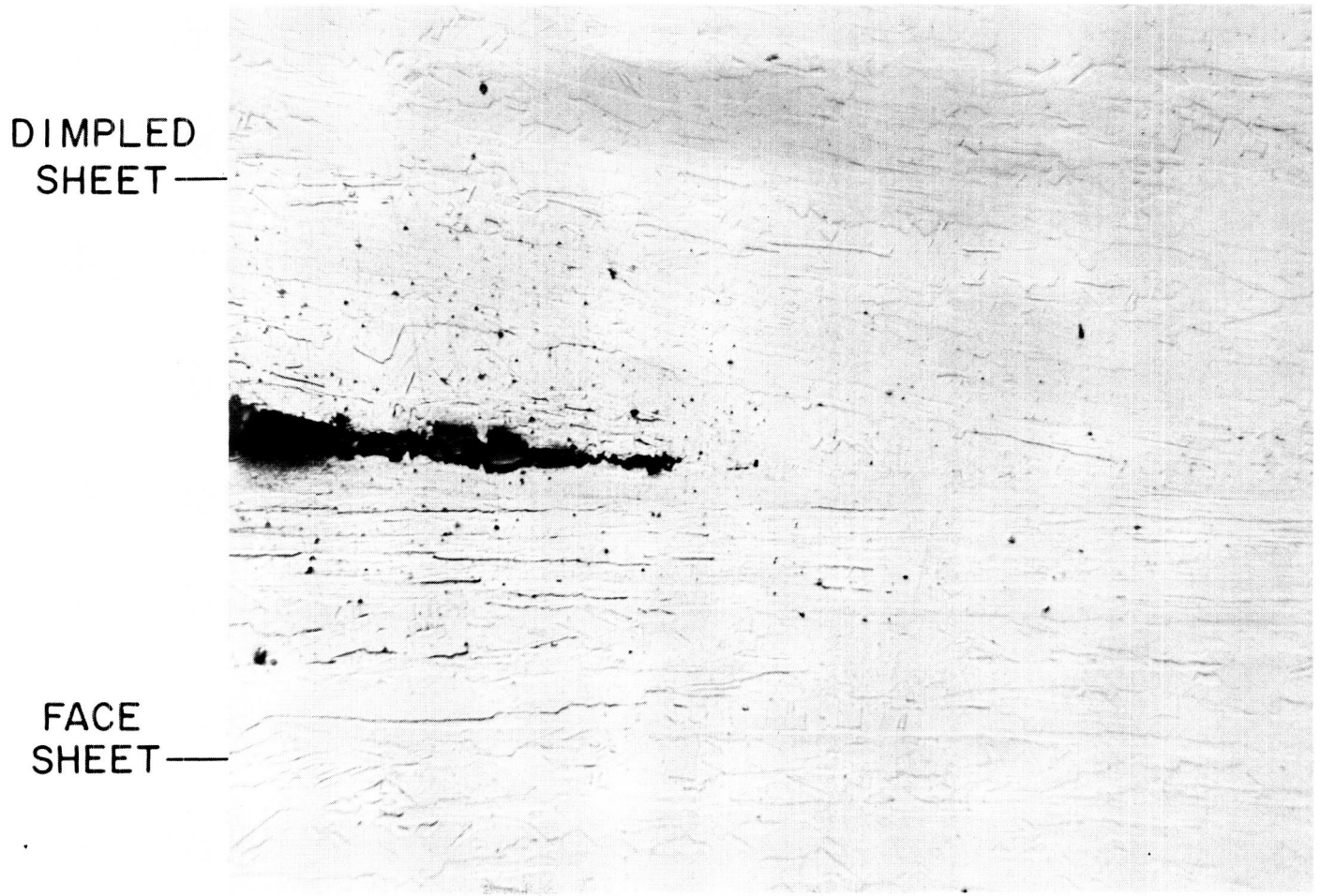

NASA

Figure 13.- Diffusion bond in TD-nickel sheet, 500×.

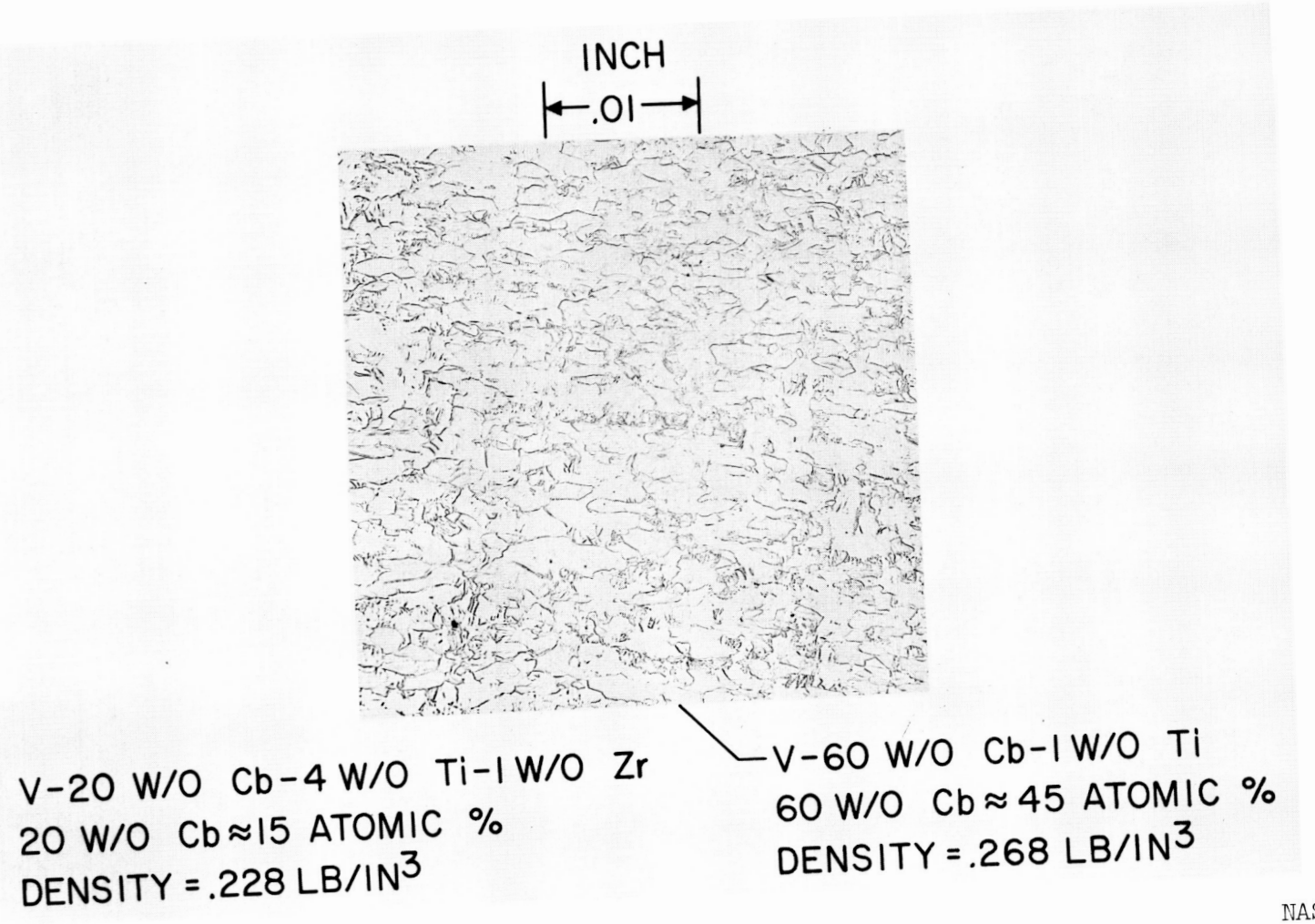

Figure 14.- Microstructure of vanadium alloy sheet.

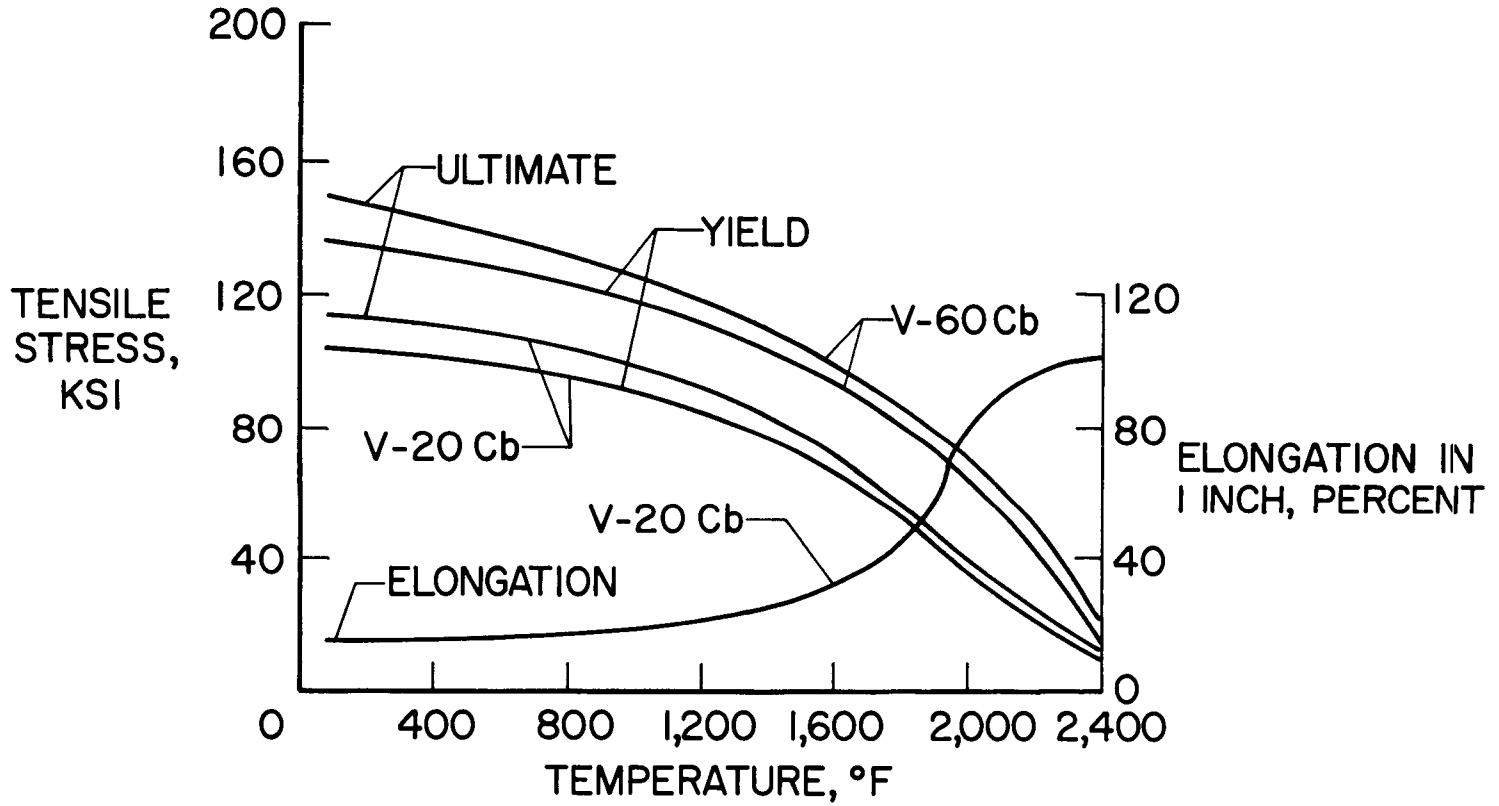

NASA

Figure 15.- Mechanical properties of V-Cb alloy sheet.

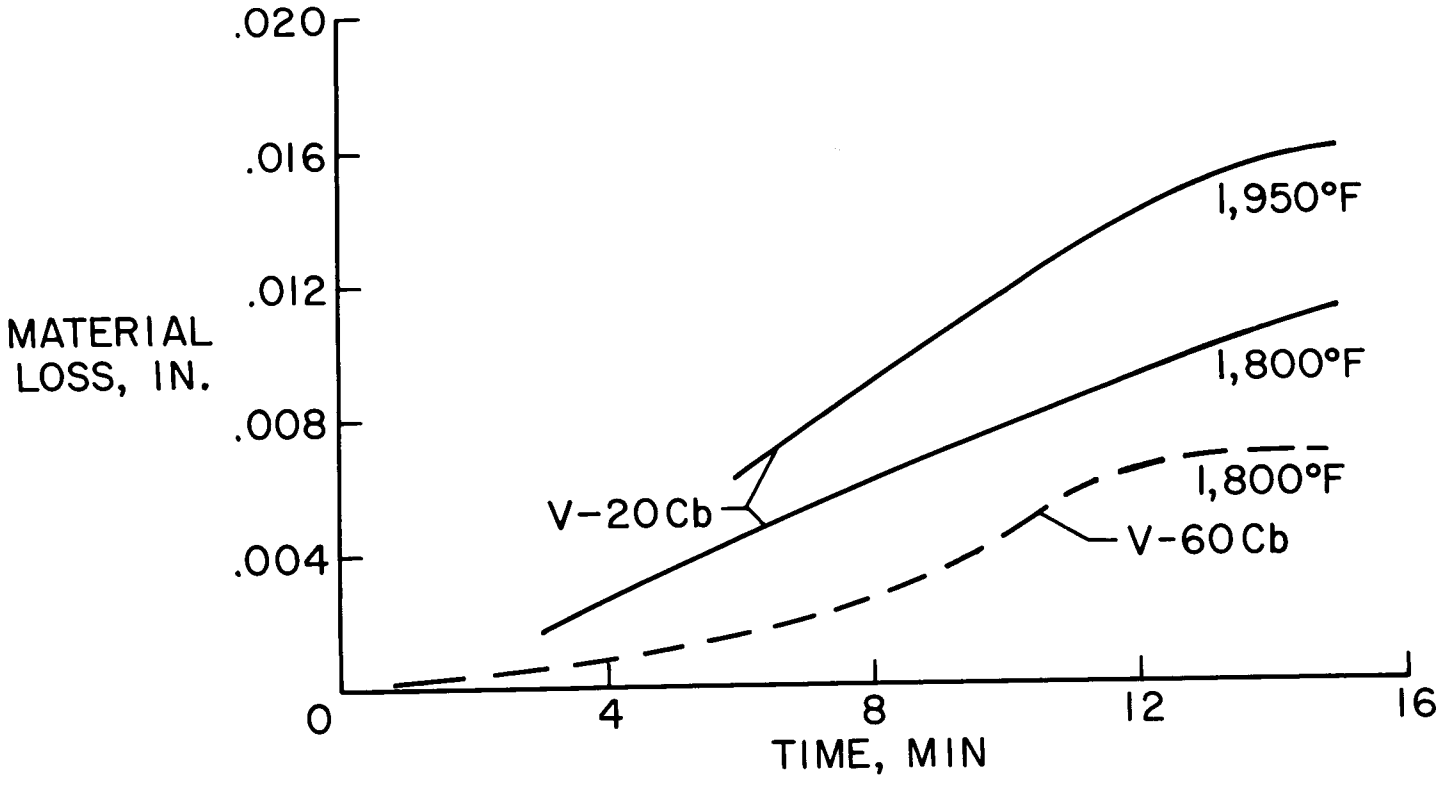

NASA

Figure 16.- Oxidation properties of V-Cb alloy sheet.

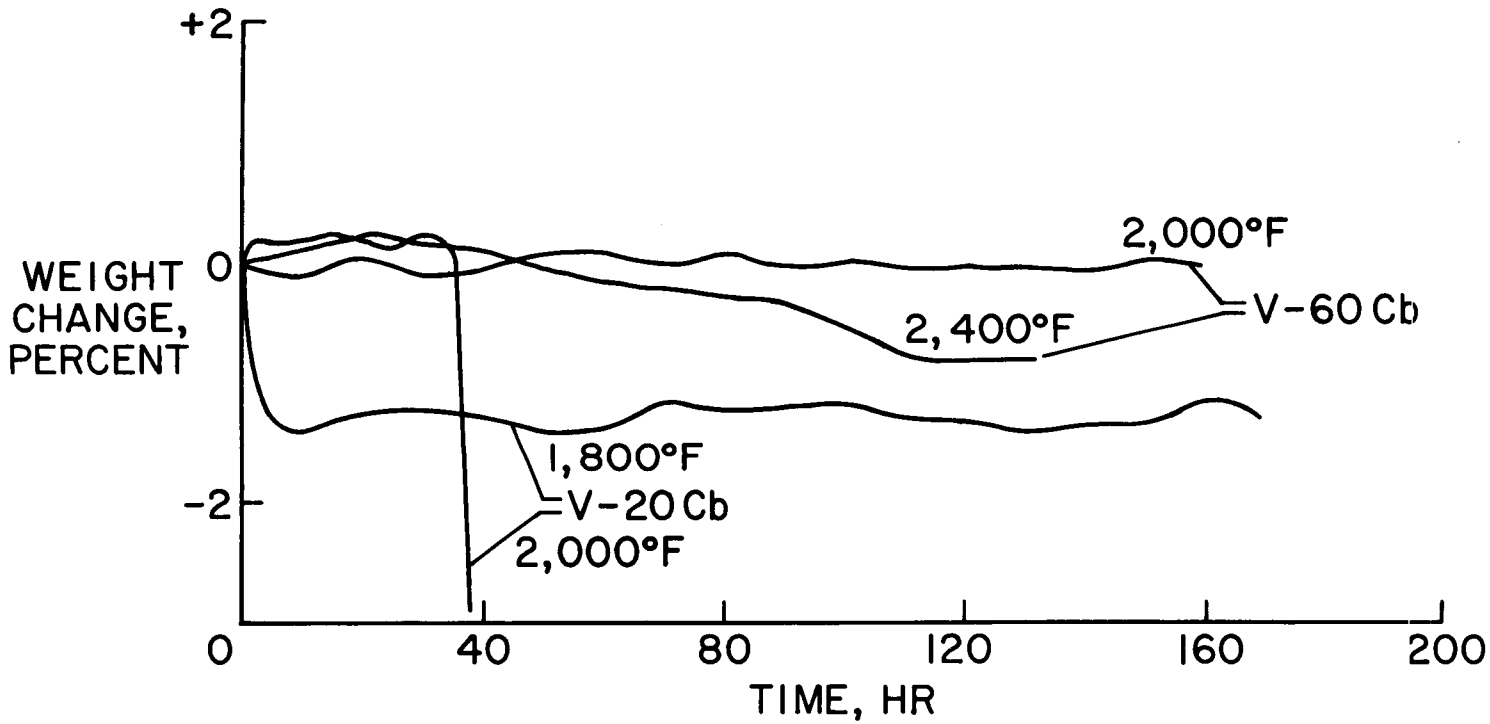

NASA

Figure 17.- Oxidation properties of V-Cb alloy sheet.

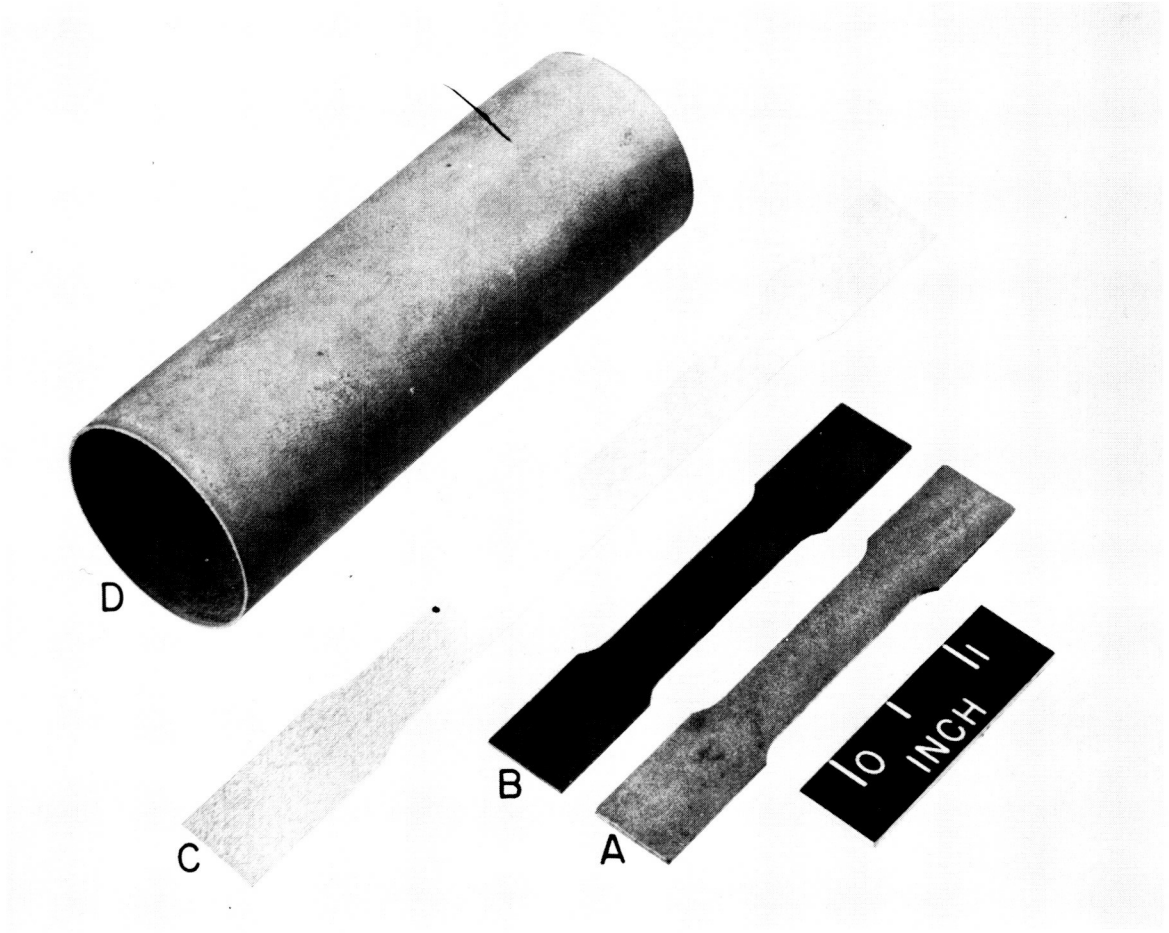

NASA

Figure 18.- Plasma-sprayed beryllium specimens.

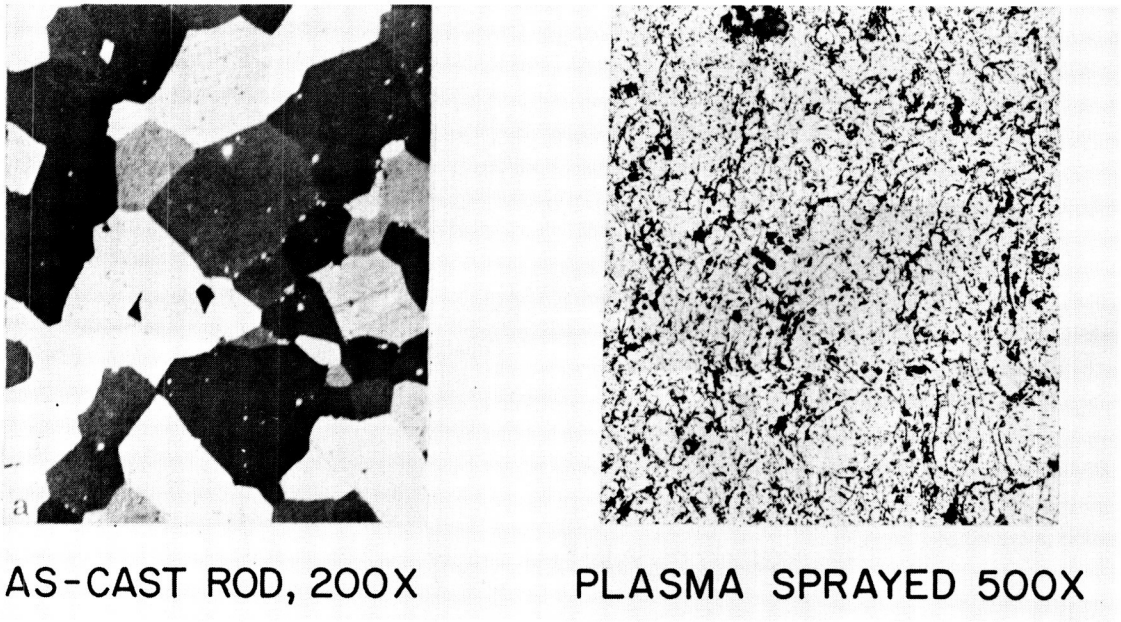

NASA

Figure 19.- Microstructure of beryllium.

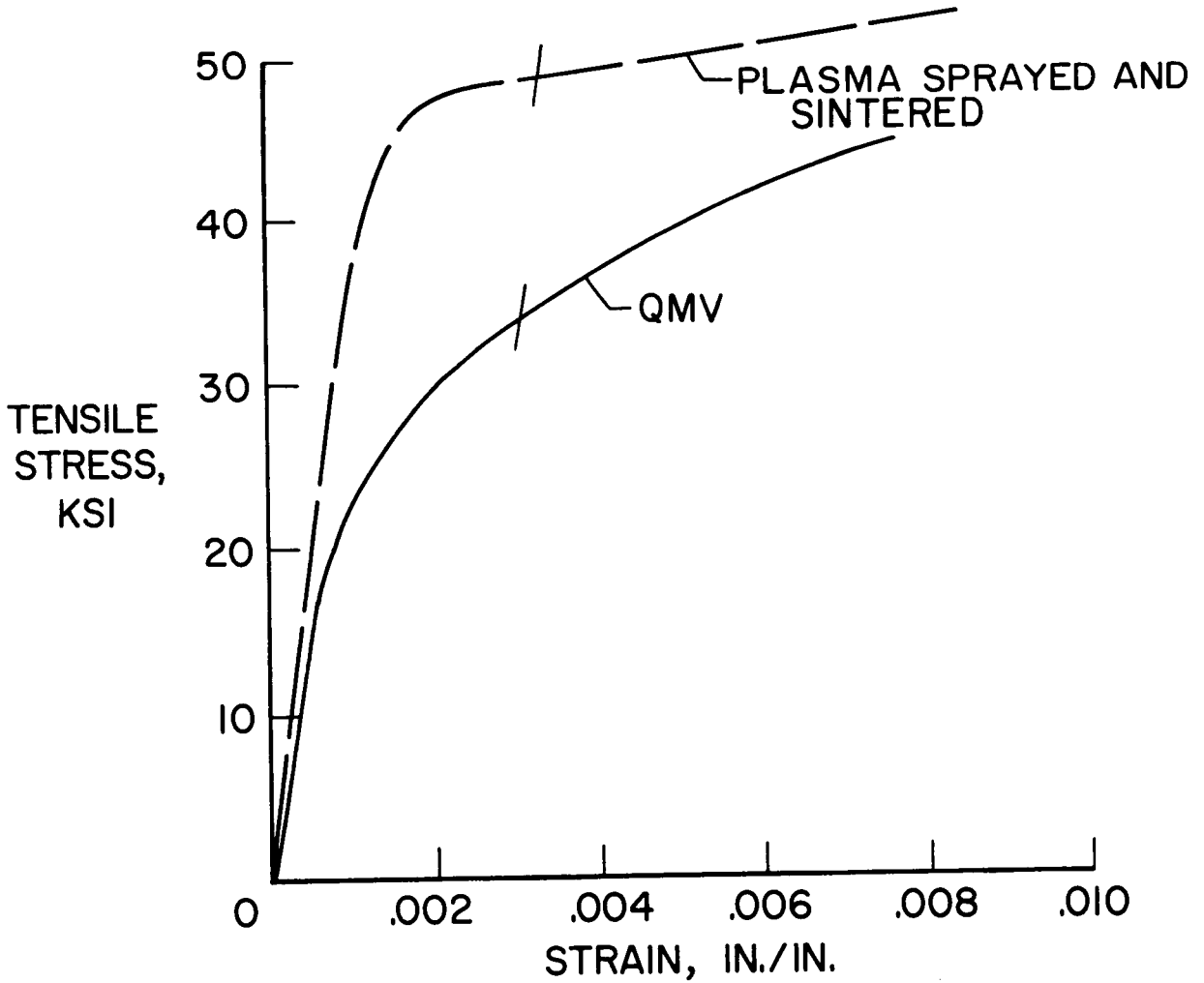

NASA

Figure 20.- Beryllium tensile stress-strain curves.